Distinctive Features of Zero Group Velocity Guided Waves for Damage Detection

YANFENG SHEN and RUNYE LU

ABSTRACT

This paper presents the recent progress from Active Materials and Intelligent Structures (AMIS) lab at Shanghai Jiao Tong University on utilizing special features of ZGV guided waves for damage detection. As the first part of this investigation, the Electro-Mechanical Impedance (EMI) method is studied, focusing on a special "trembling" phenomenon in the spectrum at the ZGV resonance. Finite Element Modeling (FEM) is performed to showcase such an interesting feature. It is found that the trembling feature following the resonance peak can serve as a special signature for ZGV modes identification and damage evaluation. Experiments on delamination detection is performed to demonstrate the superb sensitivity of the ZGV impedance technique. As the second part of this investigation, the nonlinear ZGV waves for fatigue damage detection is studied. The nonlinear interactions between guided waves and the fatigue crack generate second higher harmonics. Residing the second harmonics at the ZGV mode allows the nonlinear wave features to accumulate in the vicinity of the cracks. FEM simulations are carried out to demonstrate and analyze the special phenomenon. It is found that the second harmonic ZGV renders a much stronger nonlinear signature, which considerably enhances the damage detection sensitivity. The paper finishes with summary, concluding remarks, and suggestions for future work.

INTRODUCTION

Guided waves have been pervasively investigated in Structural Health Monitoring (SHM) and Non-destructive Evaluation (NDE) due to their long-distance coverage and damage-sensitive advantages. Zero group velocity (ZGV) modes, known as the

Yanfeng Shen, University of Michigan-Shanghai Jiao Tong University Joint Institute, Shanghai Jiao Tong University, Shanghai, 200240, China, yanfeng.shen@sjtu.edu.cn
Runye Lu, University of Michigan-Shanghai Jiao Tong University Joint Institute, Shanghai Jiao Tong University, Shanghai, 200240, China

non-propagating waves, have triggered tremendous research curiosity regarding their existence, generation, and bizarre characteristics [1]. Researchers explored the existence of ZGV modes theoretically in solids and liquids. ZGV modes are consequently endowed with peculiar attributes of a zero-group velocity with a finite nonzero wavenumber, resulting in a phase-varying wave packet under a motionless envelope [2, 3]. Such stationary modes give rise to a localized resonance in the thickness direction, confining the wave energy in the vicinity of their formation.

To take advantage of ZGV modes for structural sensing applications, their actuation, measurement, and extraction are of great significance. Various sensors have been developed and fabricated for the excitation and measurement of ZGV resonances, classified as contact and noncontact approaches, including PVDF-based transducers, electro-magnetic acoustic transducer (EMAT), accelerometer/microphone, air-coupled transducers, laser interferometers, interdigital transducer (IDT), and laser doppler vibrometers. To exemplify, Zhu et al. exploited piezoelectric wafer active sensors (PWAS) for the selective actuation of ZGV resonances and utilized Physical Acoustics NANO-30 sensor to measure temporal vibration signals at different locations [4]. The generation and reception of lamb wave ZGV modes were implemented employing a Q-switched Nd:YAG laser impulse and a heterodyne interferometer respectively by Prada et al. [5]. Su et al. achieved the ZGV resonances extraction through distributed sensing by PVDF-TrFE transducers [6].

The special features of ZGV modes lay the foundation for further application for structural sensing and SHM/NDE purposes. ZGV resonances possess superb sensitivity to a large family of structural damage types [7]. The non-contact evaluation of the deposited thin layer thickness by the shift of ZGV mode frequency signature. Many applications of ZGV modes for material properties determination have been demonstrated for elastic constant, Poisson's ratio, interfacial stiffness, and bulk acoustic wave velocity [8]. ZGV modes have also been explored to diagnose various damage types. Furthermore, the ZGV combined with nonlinearity induced harmonics through guided waves mixing was exploited for localized material degradation characterization [9]. The generation of a ZGV mode from nonlinear wave damage interactions in an elastic pate by non-collinear mixing was found [10].

This paper aims at reporting recent progress from Active Materials and Intelligent Structures (AMIS) lab at Shanghai Jiao Tong University on utilizing the special features of ZGV modes for SHM and NDE. Both linear and nonlinear ultrasonic methods will be covered. The distinctive trembling features in the Electro-Mechanical Impedance Spectroscopy (EMIS) will be demonstrated. The numerical and experimental case study will demonstrate its superior sensitivity and easiness for damage detection. ZGV modes for enhancing nonlinear ultrasonic performance will also be showcased. It was found that a half-ZGV frequency excitation will trigger strong local nonlinear resonances due to the cumulative effect.

FUNDAMENTALS OF ZGV LAMB MODES

The ZGV Lamb modes are used as a representative in this study. This section aims at introducing the fundamentals of the ZGV modes and provides the corresponding frequencies in a 1-mm thick aluminum plate as the example for investigation. The identification of ZGV modes and the determination of ZGV frequencies would be accomplished through the group velocity dispersion curves. Referring to the fundamentals of wave mechanics [23], the well-established Rayleigh-Lamb equations governing symmetric and anti-symmetric modes can be formulated as follows:

$$\frac{\tan\eta_P d}{\tan\eta_S d} = -\frac{\left(\xi^2-\eta_S^2\right)^2}{4\xi^2\eta_P\eta_S} \quad \text{(symmetric Rayleigh-Lamb equation)} \qquad (1)$$

$$\frac{\tan\eta_P d}{\tan\eta_S d} = -\frac{4\xi^2\eta_P\eta_S}{\left(\xi^2-\eta_S^2\right)^2} \quad \text{(antisymmetric Rayleigh-Lamb equation)} \qquad (2)$$

where d denotes the half plate thickness; $\eta_P^2=\omega^2/c_P^2-\xi^2, \eta_S^2=\omega^2/c_S^2-\xi^2$ and ξ signifies the wavenumber. Numerical solution of Rayleigh-Lamb equation yields the eigenvalues, $\xi_0^S,\xi_1^S,\xi_2^S,...,\xi_0^A,\xi_1^A,\xi_2^A,...$, representing the wavenumbers of the symmetric and anti-symmetric lamb wave modes. The group velocity curves can be obtained by solving the above equation and evaluating the following relation $c_g=c^2\cdot\left(c-fd\cdot\partial c/\partial(fd)\right)^{-1}$ against the frequency and half thickness product, fd.

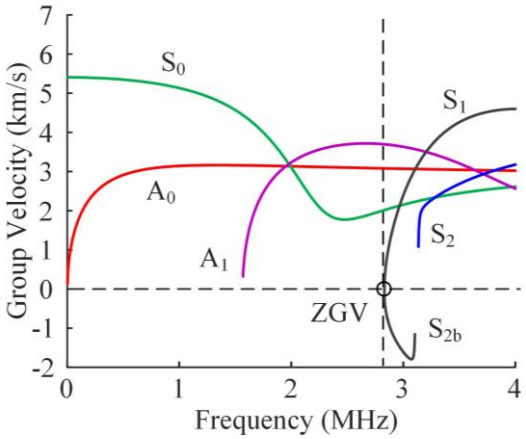

Figure 1: Typical group velocity dispersion curves for a 1-mm thick aluminum plate, showcasing the first ZGV mode.

Figure 1 presents the group velocity dispersion curves for a 1-mm thick aluminum plate. A particular location branching into the S_{2b} and S_1 modes resides in a zero-value in its group velocity. The two branches represent backward and forward propagative wave packets, while the zero-value point designates a standing and stationary resonance. The following sections will emphasize on discovering, understanding, and utilizing distinctive features of the fundamental ZGV Lamb mode for SHM and NDE.

ELECTRO-MECHANICAL IMPEDANCE AT ZGV FREQUENCIES

The EMIS method stands as a powerful approach for structural diagnostics, due to its superb sensitivity to local areas surrounding the active sensors [11]. The first part of investigation aims at revealing a special trembling feature in the EMIS signature, which could assist the identification of ZGV resonances and could be particularly useful for damage detection. Both numerical infestations and experimental demonstrations will be presented.

Numerical modeling results for demonstrating trembling features

Figure 2 presents the 2-D plain strain finite element models for investigating and showcasing the special ZGV mode feature. A 4-mm thick aluminum plate was used as the target structure. A total of four cases were investigated: single pin-force actuation for generating both symmetric and antisymmetric modes, antisymmetric pin-force actuation for antisymmetric modes generation, symmetric pin-force actuation for merely generating symmetric modes, and PWAS actuation taking the distributed coupling actuator-structural coupling effects.

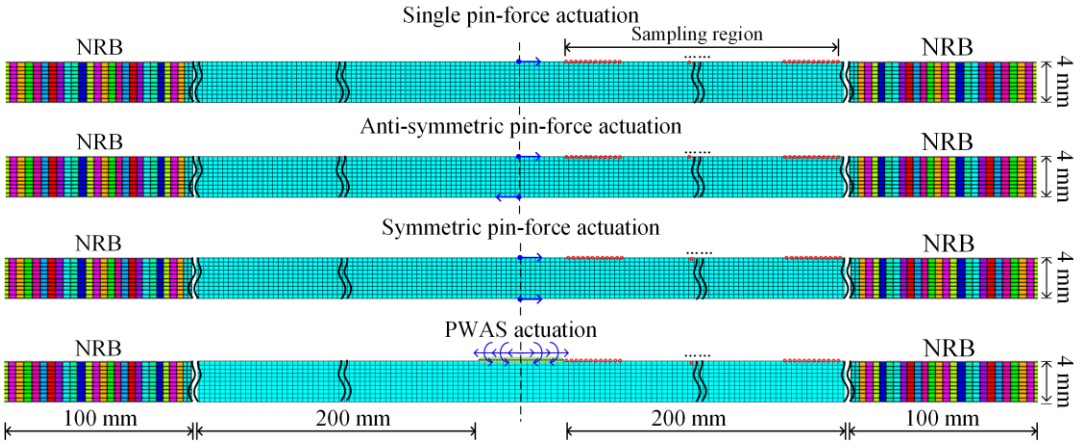

Figure 2: Finite element model setups with various actuation configurations.

Non-reflective boundary (NRB) condition was implemented at both ends of the plate to eliminate structural resonances associated with boundaries. A line of sampling points along the wave propagation direction was employed for analyzing the wave field in the plate, so that frequency-wavenumber representation could be easily obtained. A harmonic solution was captured sweeping across a band from 700 kHz to 720 kHz, covering the ZGV frequency.

Figure 3 illuminates the ZGV resonance peak for single pin-force excitation case and the PWAS actuation case. It could be noticed that following the ZGV resonance, apparent tremblings took place. This is true for both cases, regardless of the actuation physics. Such a distinctive feature does not exist for general structural resonances. Thus, it can be readily used for identification of ZGV modes, which were found to be particularly sensitive to material degradation and thickness dimension damage types like delamination, corrosion, and abrasion.

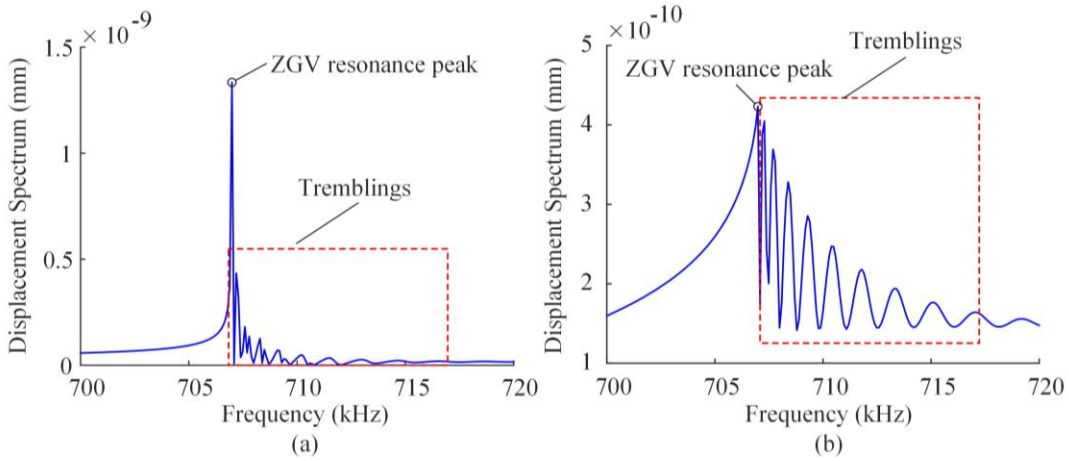

Figure 3: Comparative displacement frequency spectra for: (a) uni-direction pin-force actuation; (b) PWAS actuation under EMI framework.

On noticing the general existence of the trembling feature, it is worth looking into its association with corresponding waves modes, since Lamb waves are multi-modal by their nature. Figure 4 shows the frequency- wavenumber domain representations of the wavefields in the harmonic analyses for the antisymmetric and the symmetric pin-force actuation cases, prospectively. It can be clearly observed that antisymmetric auction only generated antisymmetric Lamb modes and they do not exhibit any trembling phenomenon, showing two smooth traces for A_0 and A_1 modes. On the other hand, the symmetric actuation generated a strong resonance at the ZGV frequency, followed by clear tremblings along both S_{2b} and S_1 branches. The S_0 mode was also excited but not influenced. Thus, such an analyses further demonstrated the distinctive feature stemming from ZGV resonances.

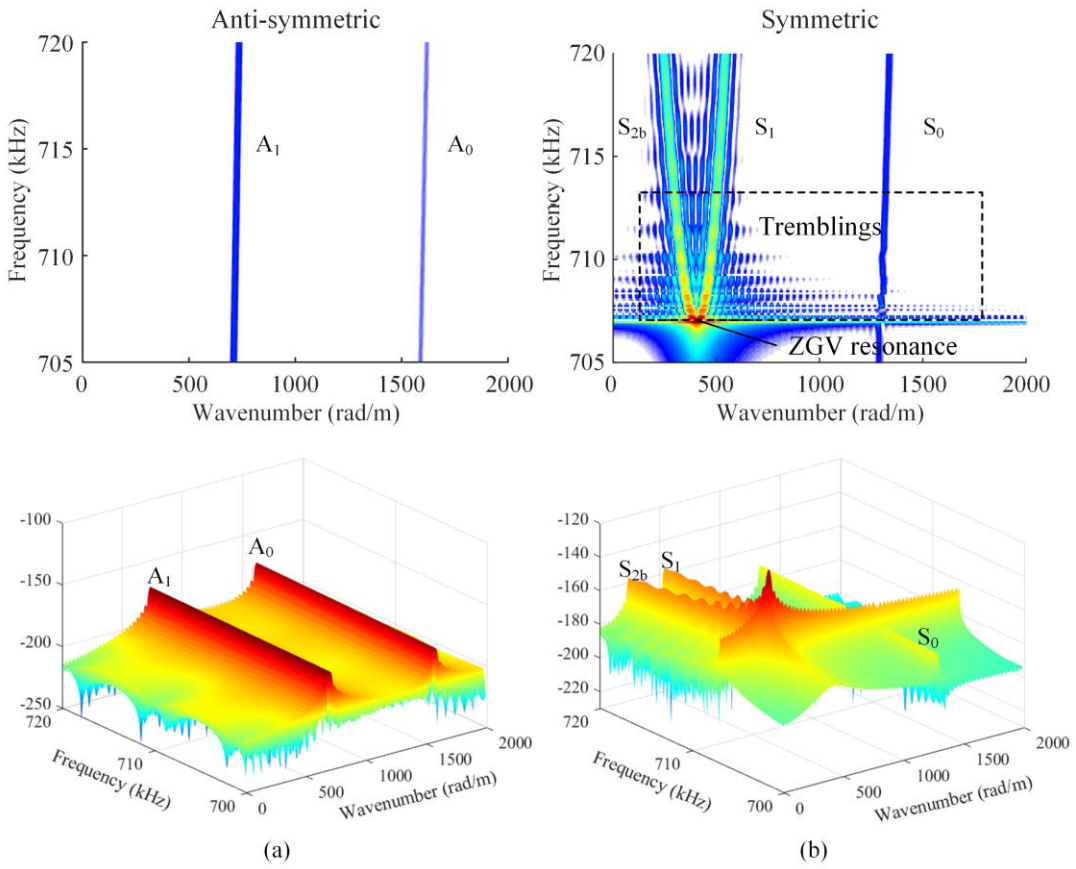

Figure 4: Dispersion curves with 3-D surface views for (a) anti-symmetric pin-force actuation and (b) symmetric pin-force actuation.

Experimental demonstration for EMIS resonances at ZGV frequencies

An experimental investigation on the distinctive trembling feature was conducted on an aluminum plate. Figure 5 presents the setup for EMIS measurement. A circular PWAS was mounted on a 4-mm thick aluminum plate surrounded by absorbing materials for eliminating boundary reflections. BODE-100 impedance analyzer was used to conduct the impedance measurement.

Figure 5 presents the impedance curves from the experiment, in comparison with FEM results. It can be noticed that a large resonance peak rises around 660 kHz, corresponding to the local resonance of the PWAS transducer. Following that, another resonance peak around 707 kHz appeared, residing at the ZGV frequency. It should be noted that right after the peak, trembling features appeared in both the experimental and FEM results. Thus, the existence of the distinctive trembling phenomenon has been substantiated. This ZVG resonance is easy to identify due to such a fact and could serve as a sensitive candidate for SHM and NDE.

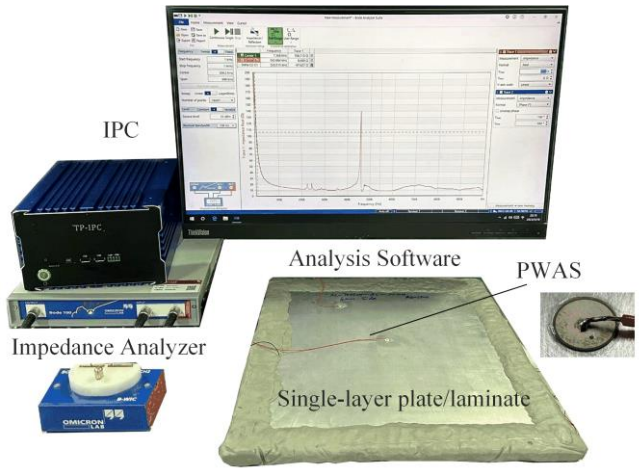

Figure 5: Experimental configurations for harmonic analysis implemented by EMIS method.

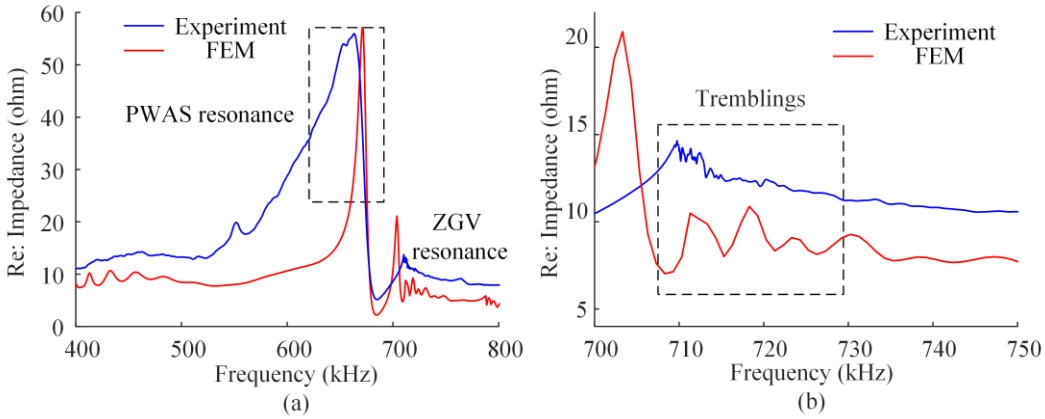

Figure 6: (a) Comparative EMI spectra from FEM and experimental analysis; (b) zoom-in view of the spectra from 700 kHz to 800 kHz (note the trembling features in both FEM and experimental measurement).

ZGV ENHANCED NONLILNEAR ULTTRASONICS

In addition to EMIS, nonlinear ultrasonics have also been widely investigated as a sensitive tool for detecting incipient fatigue cracks. However, the superharmonics generated from wave damage interactions are weak. The second part of this study focuses on leveraging the stationary and cumulative feature of ZGV modes for enhancing the sensitivity of nonlinear ultrasonic methods [12].

Numerical setup and logic for accumulative second harmonic generation

A numerical case study using the FEM shown in Figure 7 was conducted. A 1-mm thick aluminum plate was modeled with a breathing crack at the center. Both ends of the plate were implemented with NRB condition. Symmetric Lamb modes were

transmitted by a pair of symmetrically aligned pin forces. Sampling points along the wave propagation direction were deployed for analyzing the wavefield.

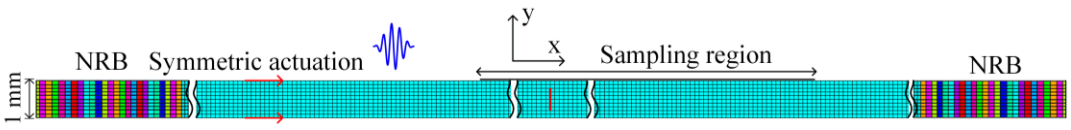

Figure 7: FE model configurations of the aluminum plate and corresponding damage settings.

The choice of wave generation frequency could make a big difference in the interrogation results, since ultrasonic based SHM and NDE techniques rely heavily on the art of careful selection of frequency and wave modes. This study particularly researched into two cases, one being a general choice of excitation frequency at 1000 kHz, while another being half-ZGV frequency (1363 kHz in this study). For the 1000 kHz excitation case, only S_0 will exist for both the fundamental frequency and the second harmonic. Even higher order of harmonics may involve in other wave modes, but will miss the ZGV point. Yet, the excitation frequency of 1363 kHz will reside the second harmonic right on the ZGV point, rendering a possibility of mode conversion from S_0 into the ZGV mode.

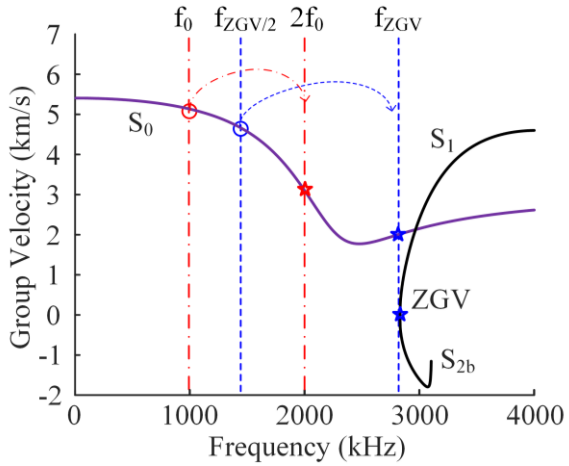

Figure 8: Selection of actuation frequencies and the corresponding second harmonic components in dispersion curves for only symmetric modes.

Enhanced sensitivity for damage detection via ZGV nonlinear ultrasonics

Figure 9 illuminates the frequency-wavenumber domain wavefield depicted by the data postprocessed from the sampling points. It can be observed that the 1000 kHz excitation case indeed generated superharmonics at 2000 kHz and 3000 kHz. But the superharmonic amplitudes are much lower that that of the fundamental frequency. On the other hand, the half-ZGV excitation frequency resulted in a strong second

harmonic response. In addition, the wavenumber analysis demonstrated that ZGV mode was generated and converted from the S_0 mode. The strong second harmonic signal stems from the stationary and cumulative feature of ZGV mode.

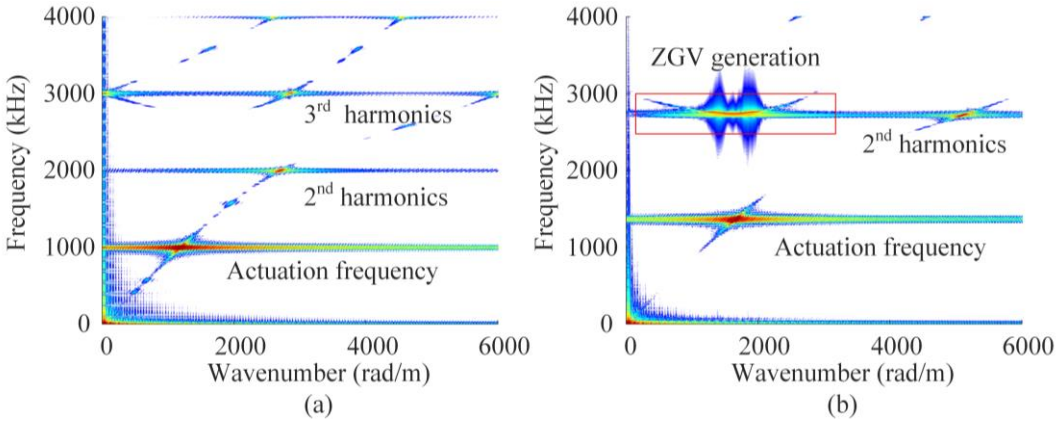

Figure 9: Wavenumber-frequency dispersion curves for (a) 1000 kHz actuation case; (b) half-ZGV frequency actuation case.

The ratio between the second harmonic amplitude and the fundamental frequency component is usually used as a measurement of the signal nonlinearity, thus reflecting and evaluating the damage severity. The stronger second harmonic one can sense, the more sensitive the nonlinear ultrasonic method could be. Figure 10 presents the spectra of sensing signals near the crack location. Both x direction and y direction displacements were used for the demonstration. It is apparent that the second harmonic achieved a much higher amplitude for the half-ZGV excitation case than that of the 1000 kHz excitation case. For y direction displacement signal, the second harmonic component was even higher than the fundamental frequency, which could not be achieved for general cases.

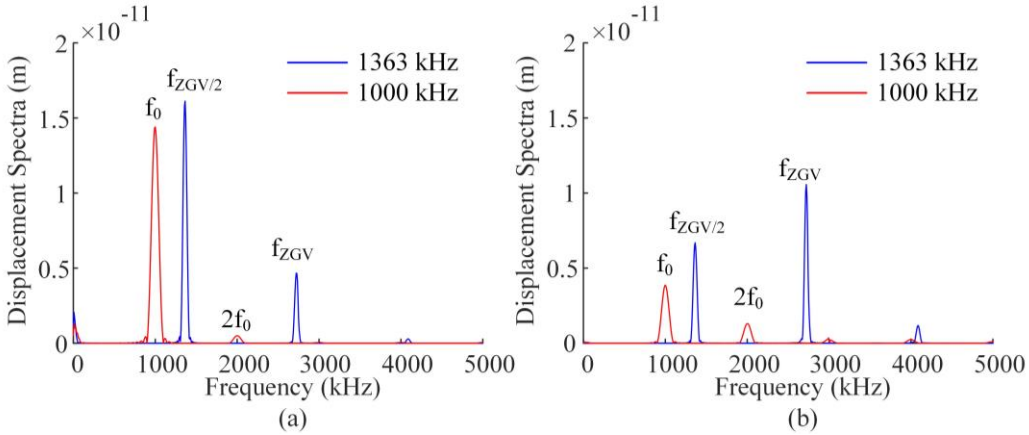

Figure 10: Comparative displacement frequency spectra for both actuations at the damage site (a) displacement in x direction; (b) displacement in y direction.

To quantify the second harmonics, a nonlinear intensity index was defined as the ratio of the second harmonic amplitude to that of the fundamental wave, represented by $\chi = A_{2f}/A_f$. The nonlinear intensity values for both actuation cases, listed in TABLE 1, further validated the enhanced performance of the ZGV resonance. It should be noted that the second harmonic amplitude increases greater than that of the fundamental frequency, rendering an intensity factor larger than 1, which is typically not achievable for conventional selection of wave modes.

TABLE 1: NONLINEAR INDEX VALUES

Frequency	X direction	Y direction
χ : 1000 kHz	0.035	0.338
χ : 1363 kHz	0.288	1.579
Increasing Rate	722.86%	367.16%

CONCLUDING REMARKS AND FUTURE WORK

This paper presented the recent progress from Active Materials and Intelligent Structures (AMIS) lab at Shanghai Jiao Tong University on utilizing special features of ZGV modes for damage detection. The first part showed that EMIS measurements at ZGV resonances presented an interesting trembling feature, which could assist identifying the ZGV resonance mode with superb sensitivity for structural degradation monitoring. The second part of the paper demonstrated the sensitivity of nonlinear ultrasonic techniques can be considerably enhanced by leveraging the ZGV mode from mode conversion at superharmonics. The stationary and cumulative effect could greatly improve the sensing capability for originally weak super harmonics.
For the future work, analytical formulation for the trembling features should be derived. Experiments on the ZGV nonlinear ultrasonics should be conducted on metallic and anisotropic composite panels.

REFERENCES

[1] C. Prada, D. Clorennec and D. Royer, "Local vibration of an elastic plate and zero-group velocity Lamb modes," *Journal of Acoustical Sociaty of America,* vol. 124, no. 1, pp. 203-212, 2008.

[2] Y. Wu, R. Cui, K. Zhang, X. Zhu and J. Popovics, "On the existence of zero-group velocity modes in free rails: Modeling and experiments," *NDT & E International,* vol. 132, 2024.

[3] X. Meng, M. Deng and W. Li, "Validation of zero-group-velocity feature guided waves in a welded joint," *Ultrasonics,* vol. 136, pp. 170-173, 2024.

[4] K. Zhang, R. Cui, Y. Wu, L. Zhang and X. Zhu, "Extraction and selective promotion of zero-group velocity and cutoff frequency resonances in bi-dimensional waveguides using the electromechanical impedance method," *Ultrasonics,* vol. 131, 023.

[5] C. Prada, O. Balogun and T. Murray, "Laser-based ultrasonic generation and detection of zero-group velocity Lamb waves in thin plates," *Applied Physics Letters,* vol. 87, 2005.

[6] Q. Liu, Y. Li, R. Guan, J. Yan, M. Liu, G. Luo, Z. Su, X. Qing and K. Wang, "Advancing measurement of zero-group-velocity Lamb waves using PVDF-TrFE transducers: first data and application to in situ health monitoring of multilayer bonded structures," *Structural Health Monitoring - An International Journal,* vol. 22, no. 4, 2022.

[7] J. Spytek, A. Ziaja-Sujdak, K. Dziedziech, L. Pieczonka, I. Pelivanov and L. Ambrozinski, "Evaluation of disbonds at various interfaces of adhesively bonded aluminum plates using all-optical excitation and detection of zero-group velcoty Lamb waves," *NDT & E International,* vol. 112, no. 1, 2020.

[8] E. Glushkov and N. Glushkova, "Multiple zero-group velocity resonances in elastic layered structures," *Journal of Sound and Vibration,* vol. 500, 2021.

[9] P. Mora, M. Chekroun, S. Raetz and V. Tournat, "Nonlinear generation of a zero group velocity mode in an elastic plate by non-collinear mixing," *Ultrasonics,* vol. 119, 2022.

[10] W. Li, C. Zhang and M. Deng, "Modeling and simulation of zero-group velocity combined harmonic generated by guided wave mixing," *Ultrasonics,* vol. 132, 2023.

[11] R. Lu, Y. Shen, B. Zhang and W. Xu, "Nonlinear Electro-Mechanical Impedance Spectroscopy for fatigue crack monitoring," *Mechanical Systems and Signal Processing,* p. 109749, 2023.

[12] R. Lu and Y. Shen, "Zero group velocity mode nonlinear ultrasonics for fatigue crack detection," *Ultrasonics,* vol. 150, 2025.